

Chapter 2

Thermodynamics of Turbochargers

2.1 Thermodynamic Characteristics

Some essential thermodynamic characteristics of gases are needed to know in the turbocharging. They are usually applied to thermodynamics of turbochargers where the charge air and exhaust gas are assumed to be compressible perfect gases [1–4].

- The total temperature T_t (K) results from the sum of the static T_s (K) and dynamic temperatures T_{dyn} (K). The static temperature is measured at the wall where the gas velocity equals zero due to the viscous boundary layer.

$$T_t = T_s + T_{dyn} = T_s + \frac{c^2}{2c_p} \quad (2.1)$$

where c is the gas velocity; c_p is the heat capacity at constant pressure.

- The total pressure p_t is calculated from the isentropic gas equation as follows:

$$p_t = p_s \left(\frac{T_t}{T_s} \right)^{\frac{\kappa}{\kappa-1}} = p_s \left(1 + \frac{\kappa-1}{2} M^2 \right)^{\frac{\kappa}{\kappa-1}} \quad (2.2)$$

where

p_s is the static pressure;
 $\kappa = c_p/c_v$ is the isentropic exponent of gas;
 M is the Mach number of gas ($M = ca$), a is the sound velocity

- The specific total enthalpy h_t results from the sum of the gas specific enthalpy and specific kinetic energy of gas.

$$h_t = h + \frac{c^2}{2} \quad (2.3)$$

where the gas specific enthalpy h (enthalpy per mass unit, J/kg) is defined as

$$\begin{aligned} h(T) &= c_p(T - T_0) + h(T_0) \\ &= u(T) + \frac{p}{\rho} = u(T) + R_g T \end{aligned} \quad (2.4a)$$

within ρ is the gas density; T_0 is the reference temperature (K); u is the specific internal energy; R_g is the gas constant; $h(T_0) \equiv 0$ at $T_0 = 0$ K ($= -273.14$ °C).

The specific internal energy u is defined as

$$u(T) - u(T_0) = c_v(T - T_0) = c_v \Delta T \quad (2.4b)$$

where $u(T_0) \equiv 0$ at $T_0 = 0$ K.

Thus, $u(T) = c_v T$; $h(T) = c_p T$; T in K.

2.2 Efficiencies of Compressor and Turbine

The compression process in the compressor is a polytropic process with increasing entropy due to friction and losses in the compressor. Figure 2.1 shows the compression process of the intake air from the state 1 at the compressor inlet (p_1, T_1) to state 2 at the compressor outlet (p_2, T_2).

The compressor efficiency η_C is defined as the ratio of the isentropic total enthalpy change from 1t to 2st to the polytropic total enthalpy change from 1t to 2t. In other words, the compressor needs more energy in the polytropic process (real process) than the possibly minimal required energy of the compressor stage in the isentropic process (ideal process) [2, 5, and 6].

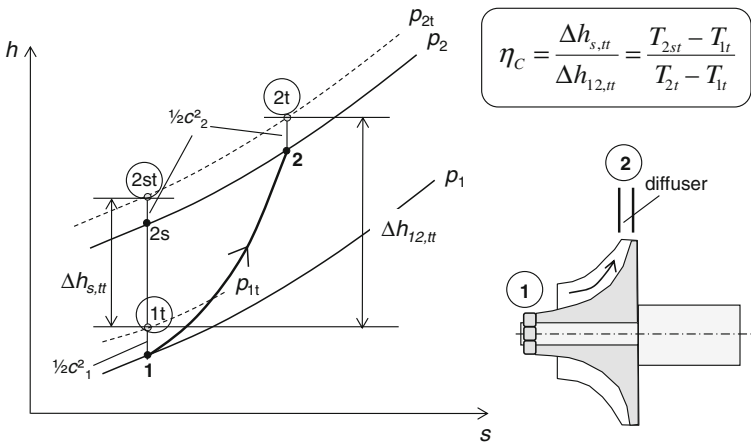


Fig. 2.1 Compression process in the compressor stage in h - s diagram

The total–total isentropic efficiency of the compressor stage (further called compressor) consisting of the compressor wheel and diffuser is defined as

$$\eta_C = \frac{\Delta h_{s,tt}}{\Delta h_{12,tt}} = \frac{T_{2st} - T_{1t}}{T_{2t} - T_{1t}} \quad (2.5)$$

The total–total isentropic efficiency is generally used in the compressor since the kinetic energy of gas in the state 2 could be transformed into the pressure energy in the diffuser. The process increases the charge-air pressure.

Using thermodynamic equations for the isentropic process, the compressor efficiency is written in terms of the total pressures and temperatures at the inlet and outlet of the compressor, and the isentropic exponent of the charge air $\kappa_a \approx 1.4$.

$$\eta_C = \frac{\left(\frac{p_{2t}}{p_{1t}}\right)^{\left(\frac{\kappa-1}{\kappa}\right)_a} - 1}{\left(\frac{T_{2t}}{T_{1t}}\right) - 1} \quad (2.6)$$

The compressor efficiency is determined by measuring the total pressures and temperatures at the inlet and outlet of the compressor according to Eq. (2.6). The maximum total–total isentropic efficiency of the compressor η_C is normally between 70 and 80 % at the design point in the compressor performance map.

Analogous to the compressor, the efficiency of turbine results from the polytropic expansion process of the exhaust gas from the state 3 at the turbine inlet (p_3, T_3) to state 4 at the turbine outlet (p_4, T_4), see Fig. 2.2. The turbine efficiency η_T is defined as the ratio of the polytropic total enthalpy change from 3t to 4t to the isentropic total enthalpy change from 3t to 4s. Physically speaking, the turbine delivers less output energy due to friction and losses in the polytropic expansion process than the possibly maximum energy given in the isentropic process.

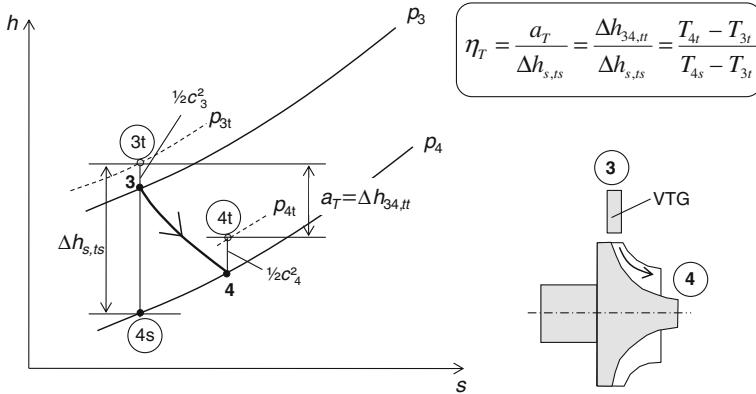


Fig. 2.2 Expansion process in the turbine stage in h - s diagram

The total-static isentropic efficiency of the turbine stage (further called turbine) consisting of the turbine wheel and variable turbine geometry (VTG) or waste gate (WG) is defined as [1, 3]

$$\eta_T = \frac{\Delta h_{34,tt}}{\Delta h_{s,ts}} = \frac{T_{4t} - T_{3t}}{T_{4s} - T_{3t}} \quad (2.7)$$

The total-static isentropic efficiency is normally used in the turbine since the kinetic energy of the exhaust gas in the state 4 does not generate any additional power for the turbine.

Applying thermodynamic equations to the isentropic process, the turbine efficiency is expressed in terms of the total pressure and temperature at the turbine inlet and outlet and the isentropic exponent of the exhaust gas $\kappa_g \approx 1.32$.

$$\eta_T = \frac{1 - \left(\frac{T_{4t}}{T_{3t}}\right)}{1 - \left(\frac{p_{4s}}{p_{3t}}\right)^{\left(\frac{\kappa-1}{\kappa}\right)_g}} \quad (2.8)$$

The turbine efficiency is determined by measuring the total pressure and temperature at the turbine inlet and outlet according to Eq. (2.8). The maximum total-static isentropic efficiency of the turbine η_T is normally between 65 and 70 % at the design point of the turbine performance map [5–7].

2.3 Turbocharger Equations

The turbocharger consists of the turbine, compressor, and core unit (CHRA: center housing and rotating assembly) including the rotor and bearing system. Both turbine and compressor wheels are fixed in the rotor shaft that is supported on the bearing system of the radial and thrust bearings. The rotating shaft including the compressor wheel, turbine wheel, thrust rings, radial bearings, and seal rings is called the *rotor* of the turbocharger.

Due to expanding the exhaust gas of the engine in the turbine, it generates the turbine power that depends on the mass flow rate of the exhaust gas through the turbine and the isentropic enthalpy drop in the turbine. The effective turbine power results as

$$P_T = \eta_T \dot{m}_T |\Delta h_{sT}| \quad (2.9)$$

The isentropic enthalpy drop in the turbine stage is calculated using thermodynamic equations.

$$|\Delta h_{sT}| = c_{p,g} T_3 \left[1 - \left(\frac{p_4}{p_3} \right)^{\left(\frac{\kappa-1}{\kappa} \right)_g} \right] \quad (2.10)$$

Inserting Eq. (2.10) into Eq. (2.9), one obtains the effective turbine power in function of the mass flow rate, inlet temperature, and pressure ratio of the turbine.

$$P_T = \eta_T P_{T,ideal} \equiv \eta_T \dot{m}_T c_{p,g} T_3 \left[1 - \left(\frac{p_4}{p_3} \right)^{\left(\frac{\kappa-1}{\kappa} \right)_g} \right] \quad (2.11)$$

Due to the friction loss in the bearing system, the required compressor power results from the effective turbine power and mechanical efficiency η_m .

$$P_C = \eta_m P_T = \eta_m \eta_T \dot{m}_T c_{p,g} T_3 \left[1 - \left(\frac{p_4}{p_3} \right)^{\left(\frac{\kappa-1}{\kappa} \right)_g} \right] \quad (2.12)$$

Analogously, the required compressor power is calculated from the isentropic compressor power and compressor efficiency.

$$P_C = \frac{P_{C,ideal}}{\eta_C} \equiv \frac{\dot{m}_C \Delta h_{sC}}{\eta_C} \quad (2.13)$$

where Δh_{sC} is the increase of the isentropic enthalpy in the compressor.

Using thermodynamic equations for an isentropic process, the required compressor power is calculated from the mass flow rate, inlet temperature, and pressure ratio of the compressor.

$$P_C = \frac{\dot{m}_C c_{p,a} T_1}{\eta_C} \left[\left(\frac{p_2}{p_1} \right)^{\left(\frac{\kappa-1}{\kappa} \right)_a} - 1 \right] \quad (2.14)$$

Substituting Eqs. (2.12 and 2.14), one obtains the pressure ratio of compressor π_C in the first turbocharger equation.

$$\begin{aligned} \pi_C = \frac{p_2}{p_1} &= \left(1 + \frac{c_{p,g}}{c_{p,a}} \left\langle \frac{\dot{m}_T T_3}{\dot{m}_C T_1} \eta_{TC} \right\rangle \cdot \left[1 - \left(\frac{p_3}{p_4} \right)^{-\left(\frac{\kappa-1}{\kappa} \right)_g} \right] \right)^{\left(\frac{\kappa}{\kappa-1} \right)_a} \\ &= \left(1 + \frac{c_{p,g}}{c_{p,a}} \left\langle \frac{\dot{m}_T T_3}{\dot{m}_C T_1} \eta_{TC} \right\rangle \cdot \left[1 - \pi_T^{-\left(\frac{\kappa-1}{\kappa} \right)_g} \right] \right)^{\left(\frac{\kappa}{\kappa-1} \right)_a} \end{aligned} \quad (2.15)$$

within the overall efficiency of the turbocharger η_{TC} is written as

$$\eta_{TC} = \eta_m \eta_T \eta_C \quad (2.16)$$

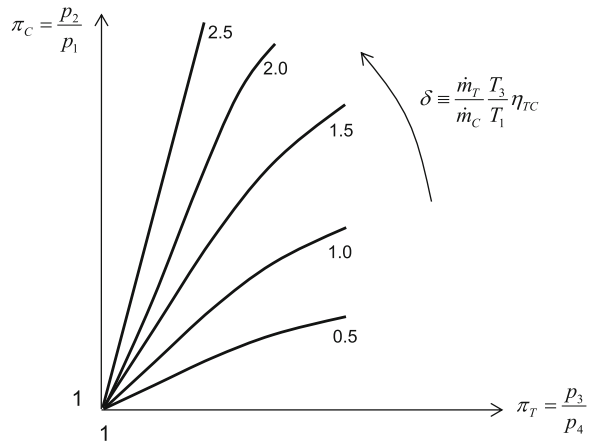
To achieve the high boost pressure of the charge air p_2 , the compressor pressure ratio π_C could be improved according to Eq. (2.15) if

- the overall turbocharger efficiency η_{TC} is high, especially a high mechanical efficiency of the bearing system in low-end torque;
- the exhaust gas temperature T_3 is high due to the large enthalpy. Hence, more turbine power is generated;
- the turbine pressure ratio π_T (turbine expansion ratio) is as high as possible;
- the inlet air temperature T_1 is as low as possible; therefore, the charge-air temperature T_2 is low leading to a high density of the charge air;
- the exhaust gas pressure p_3 is chosen at an optimal pressure in order to compromise between the turbine power and specific fuel consumption;
- the exhaust gas mass flow rate in the turbine should be large.

The first turbocharger Eq. (2.15) shows the behavior of the pressure ratio $\pi_C (\equiv p_2/p_1)$ of the compressor versus the pressure ratio $\pi_T (\equiv p_3/p_4)$ of the turbine. In fact, the dimensionless term δ in the angle brackets $\langle \rangle$ of Eq. (2.15) does not change so much along the full load curve in the compressor performance map. Therefore, the behavior of the pressure ratios of turbine and compressor can be displayed at various dimensionless parameters δ in Fig. 2.3.

The exhaust gas flow in the turbine can be considered as a compressible flow in a nozzle in which the inlet and outlet pressures are p_3 and p_4 , respectively. Based on the flow equation for compressible fluids in the nozzle, the *second turbocharger equation* describes the mass flow rate through the turbine in function of the pressure, temperature at the turbine inlet, and the turbine expansion ratio.

Fig. 2.3 Behavior of the pressure ratios π_C versus π_T



$$\dot{m}_T = \mu A_T p_{3t} \sqrt{\frac{2}{R_g T_{3t}}} \sqrt{\left(\frac{\kappa}{\kappa - 1}\right)_g \left(\left(\frac{p_{3t}}{p_4}\right)^{\frac{2}{\kappa_g}} - \left(\frac{p_{3t}}{p_4}\right)^{-\left(\frac{\kappa+1}{\kappa}\right)_g} \right)} \quad (2.17)$$

where μ is the flow coefficient due friction and flow contraction at the nozzle outlet, A_T is the throttle cross-sectional area in the turbine wheel.

To eliminate the influences of p_{3t} and T_{3t} on the mass flow rate in the turbine shown in Eq. (2.17), the so-called corrected mass flow rate is defined as

$$\begin{aligned} \dot{m}_{T,cor} &\equiv \frac{\dot{m}_T \sqrt{T_{3t}}}{p_{3t}} = f(\pi_{T,ts}) \\ &= \mu A_T \sqrt{\frac{2}{R_g}} \sqrt{\left(\frac{\kappa}{\kappa - 1}\right)_g \left(\left(\frac{p_{3t}}{p_4}\right)^{\frac{2}{\kappa_g}} - \left(\frac{p_{3t}}{p_4}\right)^{-\left(\frac{\kappa+1}{\kappa}\right)_g} \right)} \end{aligned} \quad (2.18)$$

Equation (2.18) indicates that the corrected mass flow rate of the turbine is independent of the inlet condition of the exhaust gas of p_{3t} and T_{3t} . It depends only on the turbine expansion ratio $\pi_{T,ts}$.

The performance map of the turbine displays the corrected mass flow rate over the turbine expansion ratio $\pi_{T,ts}$ at various rotor speeds in Fig. 2.4. From a turbine pressure ratio of approximately 3, the mass flow rate has no longer increased, even at higher rotor speeds. In this case, the flow in the turbine becomes a choked flow in which the exhaust gas speed at the throttle area reaches the sonic speed with Mach number $M = 1$. As a result, the exhaust gas mass flow rate through the turbine corresponding to the nominal engine power must be smaller than the mass flow rate

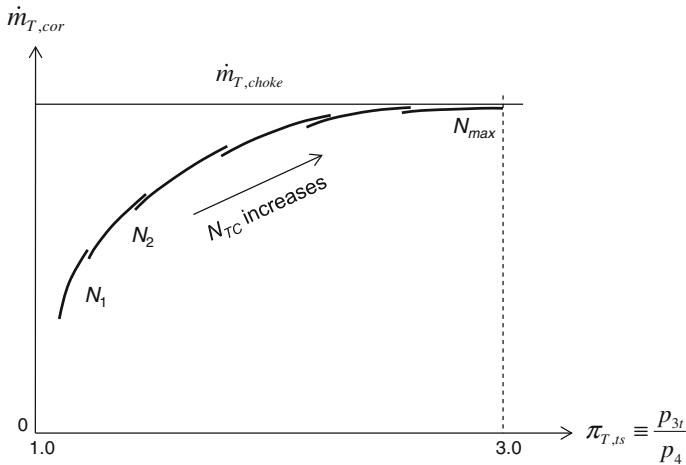


Fig. 2.4 Performance map of the turbine

at choke. Note that the isentropic turbine efficiency at the choked flow is extremely low ($\eta_T < 60\%$). This low efficiency is unusable in the automotive turbochargers.

The mechanical efficiency of turbocharger induced by the bearing friction results from Eq. (2.12).

$$\eta_m = \frac{P_C}{P_T} = \frac{\dot{m}_C c_{p,a} (T_2 - T_1)}{\eta_C \eta_T \dot{m}_T c_{p,g} T_3 \left[1 - \left(\frac{p_4}{p_3} \right)^{\left(\frac{\kappa-1}{\kappa} \right)_g} \right]} \quad (2.19)$$

Using Eqs. (2.14 and 2.19), the efficiency product of the mechanical and turbine efficiencies is written as

$$\eta_m \eta_T = \frac{\dot{m}_C c_{p,a} T_1 \left[\left(\frac{p_2}{p_1} \right)^{\left(\frac{\kappa-1}{\kappa} \right)_a} - 1 \right]}{\eta_C \dot{m}_T c_{p,g} T_3 \left[1 - \left(\frac{p_3}{p_4} \right)^{-\left(\frac{\kappa-1}{\kappa} \right)_g} \right]} \quad (2.20)$$

The efficiency $\eta_m \eta_T$ described in Eq. (2.20) is a key part in the overall efficiency of the turbocharger. It is determined by measuring the thermodynamic characteristics in Eq. (2.20), such as the mass flow rates in the compressor and turbine, temperatures T_1 and T_3 , compressor efficiency η_C , pressures at the compressor inlet and outlet p_1 and p_2 , and as well as pressures at the turbine inlet and outlet p_3 and p_4 . Figure 2.5 displays the efficiency $\eta_m \eta_T$ versus pressure ratio of turbine $\pi_{T,ts}$ at various rotor speeds.

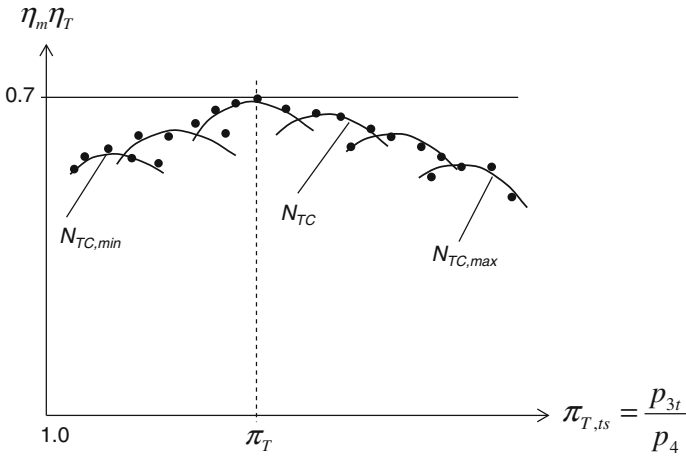


Fig. 2.5 Efficiency $\eta_m \eta_T$ versus $\pi_{T,ts}$ at various rotor speeds N_{TC}

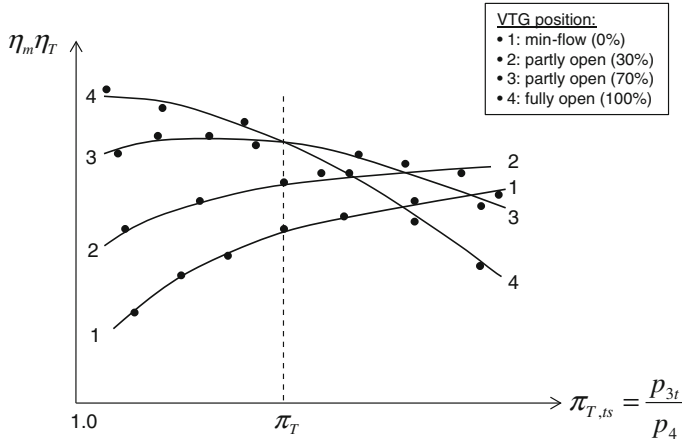


Fig. 2.6 Efficiency $\eta_m\eta_T$ versus $\pi_{T,ts}$ at various VTG positions

At low rotor speeds corresponding to the low-pressure expansion ratios π_T , the mechanical efficiency is quite small due to large bearing friction at the low oil temperature in the bearings. Additionally, the turbine efficiency is still small due to the aerodynamic operating condition at the low rotor speed. Therefore, the resulting efficiency $\eta_m\eta_T$ remains low.

At high rotor speeds, the mechanical efficiency of the bearings increases due to the increased oil temperature and therefore less friction in the bearings. As a result, the efficiency $\eta_m\eta_T$ reaches a maximum value at the turbine pressure ratio at the design point in the performance map.

As the rotor speed further increases to the maximum speed, the turbine efficiency drops due to the aerodynamic operating condition at high rotor speeds; the mechanical efficiency decreases because the bearing friction rises at high rotor speeds. Therefore, the efficiency $\eta_m\eta_T$ decreases with the rotor speed corresponding to the turbine pressure ratio.

However, the efficiency $\eta_m\eta_T$ depends not only on the turbine pressure ratio but also on the position of VTG (variable turbine geometry), as shown in Fig. 2.6.

- Initially, the VTG is open at the min-flow condition for the minimum mass flow rate called 0 % VTG (position 1) at the idle condition of the engine. The efficiency $\eta_m\eta_T$ increases with the turbine pressure ratio because the turbine efficiency becomes larger at high mass flow rates corresponding to a high turbine pressure ratio.
- The VTG begins opening at 30 % VTG (position 2). At increasing turbine pressure ratios, the mass flow rate of exhaust gas rises in the turbine leading to the high turbine efficiency. Hence, the efficiency $\eta_m\eta_T$ increases since the turbine pressure ratio rises to the pressure ratio π_T at the design point, as shown in Fig. 2.5. As a result, the efficiency $\eta_m\eta_T$ is higher than the efficiency at the position 1.

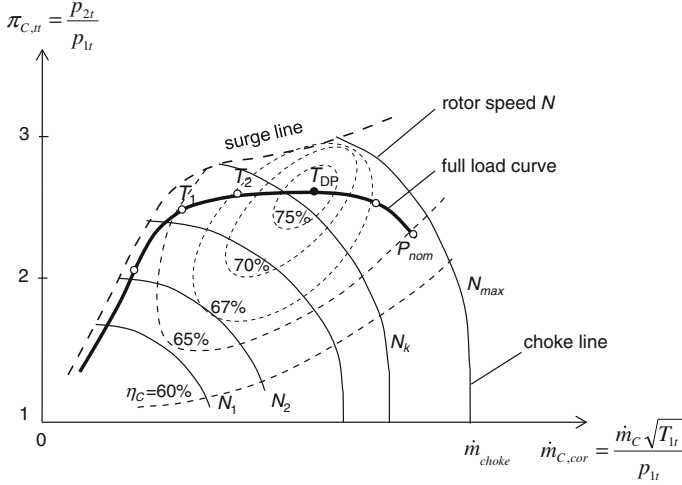


Fig. 2.7 Compressor performance map

- At the position of 70 % VTG (position 3), the turbine efficiency begins decreasing at high mass flow rates corresponding to large turbine pressure ratios.
- Finally, the VTG is fully open at 100 % VTG (position 4). The mass flow rate significantly increases in the turbine at increasing turbine pressure ratio. Therefore, the turbine efficiency reduces with the turbine pressure ratio. As a result, the efficiency $\eta_m \eta_T$ drops with the turbine pressure ratio.

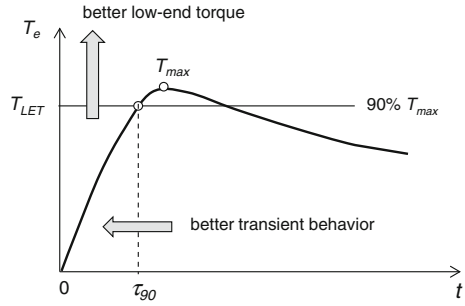
The compressor performance map in Fig. 2.7 shows the compressor ratio π_c versus the corrected mass flow rate.

At low rotor speed in the idle condition of about 30 % of the maximum rotor speed N_{max} , the compressor pressure ratio on the full load curve increases strongly with the mass flow rate to deliver a good transient response at low-end torque. At further increasing the rotor speed N to nearly 70 % of N_{max} , the compressor pressure ratio increases to approximately 2.5 and the engine achieves the maximum torque from T_1 to the design point T_{DP} . Due to the reduced turbine efficiency at the high rotor speeds leading to reducing the overall efficiency of the turbocharger, the compressor pressure ratio decreases at the nominal engine power P_{nom} in the full load curve according to the first turbocharger Eq. (2.15).

2.4 Response Time of Turbochargers

The response time is an important characteristic dealing with turbolag in automotive turbochargers. The turbolag is the delayed time that the turbocharger needs to reach the maximum engine torque from the idle.

Fig. 2.8 Response time of a turbocharger



To characterize the turbolag of the turbocharger, the response time τ_{90} is defined by the time interval that is required to reach the low-end torque (LET) T_{LET} of 90 % of the maximum engine torque T_{max} in low-end torque LET (see Fig. 2.8). The response time τ_{90} results from the effective turbine power and the polar mass inertia moment of the rotor.

Note that the better the transient behavior of the turbocharger is, the shorter the response time τ_{90} is at a given LET. The better the LET is, the higher the LET T_{LET} is at a given response time.

The angular acceleration of the rotor is calculated from the turbocharger dynamics equation.

$$\eta_m P_T - P_C = I_p \ddot{\theta} \Omega \quad (2.21)$$

The mechanical efficiency of the bearing is calculated as [4]

$$\eta_m = 1 - \frac{P_{fB}}{P_T} \quad (2.22)$$

where P_{fB} is the bearing friction power.

The rotor speed N_{TC} of the turbocharger results from Eqs. (2.21 and 2.22) in

$$N_{TC} = \frac{\Omega}{2\pi} = \frac{(\eta_m P_T - P_C)}{2\pi I_p \ddot{\theta}} = \frac{(P_T - P_{fB} - P_C)}{2\pi I_p \ddot{\theta}} \quad (2.23)$$

Integrating with time the angular acceleration within the response time τ_{90} , one obtains the average angular rotor velocity in LET

$$\Omega_{90} = \int_0^{\tau_{90}} \ddot{\theta}(t) dt \approx \bar{\ddot{\theta}} \tau_{90} \quad (2.24)$$

where $\bar{\ddot{\theta}}$ is the average angular acceleration within the response time.

Substituting Eq. (2.24) into Eq. (2.21) and eliminating the average angular acceleration, the response time of the turbocharger results in

$$\tau_{90} \approx \frac{I_p \Omega_{90}^2}{(\eta_m P_T - P_C)} = \frac{4\pi^2 I_p N_{90}^2}{(\eta_m P_T - P_C)} \quad (2.25)$$

where

I_p is the polar mass inertia moment of the rotor;

P_T is the effective turbine power;

P_C is the effective compressor power;

η_m is the mechanical efficiency of the bearings.

In order to have a good transient response of the turbocharger, it is necessary to keep the response time τ_{90} as small as possible at a given rotor speed N_{90} . According to Eq. (2.25), since the effective turbine power P_T is relatively small in LET, the response time τ_{90} rises leading to a large turbolag of the turbocharger. However, there are some improving measures:

(1) The polar mass inertia moment I_p of the rotor should be as small as possible. The turbine wheel plays a key role in the entire polar mass inertia moment of the rotor due to its heavy mass of Inconel 713C. The polar mass inertia moment of the turbine wheel is proportional to its mass m and squared wheel diameter D^2 . Due to $m \sim \rho D^3$, the polar mass inertia moment of the rotor is written as

$$\begin{aligned} I_p &\approx I_{p,TW} \propto m D^2 \\ &\propto \rho D^5 \end{aligned} \quad (2.26)$$

To reduce the inertia moment of the turbine wheel, there are some possibilities as follows:

- The turbine wheel should be as light as possible, such as using light titanium aluminide TiAl6V4 ($\rho = 4.45 \text{ g/cm}^3$) instead of heavy Inconel 713C ($\rho = 7.91 \text{ g/cm}^3$);
- The turbine wheel is scalloped at the back face to reduce its mass. However, the turbine efficiency could be reduced by 2–3 % due to the unsuitable aerodynamic flow at the scalloped back face leading to a reduction of the effective turbine power according to Eq. (2.11);
- The inflow diameter D of the turbine wheel should be reduced in order to decrease the polar inertia moment and to increase the turbine efficiency at low rotor speeds leading to the increase of the effective turbine power. However, the small turbine wheel has some negative effects, such as low turbine efficiency at high rotor speeds and small mass flow rate. As a result, the nominal turbine power is reduced.

(2) The mechanical efficiency η_m should be increased using airfoil bearings, magnetic bearings, rolling-element bearings, or rotating floating ring bearings with two oil

films. Generally, the rolling-element bearings generate less friction power, especially in LET. Contrary to the ball bearings, oil-film bearings induce a little more friction power in LET since the oil viscosity in the bearing is high at low rotor speeds.

In fact, the ratio of the bearing friction to turbine power is relatively high in LET due to the small effective turbine power and high bearing friction. However, the discrepancy between the friction coefficients of the rolling element and rotating floating ring bearings is negligibly small at high rotor speeds. Note that the rolling-element bearings cost about 10 times of the oil-film bearings. Therefore, it is recommended to carefully decide which material of the turbine wheel should be used, the suitable inflow diameter of the turbine wheel, either scalloped or unscalloped turbine wheel. Furthermore, which bearing system should be used in the turbochargers in compromise between the transient response and cost of the bearings?

2.5 Turbocharger Matching

The matching procedure of turbochargers based on the engine characteristics, compressor performance map, turbine performance map, and first turbocharger equation is discussed in the following section (see Fig. 2.9).

The following steps are carried out for the matching procedure of turbochargers [5–7]:

(1) From the engine characteristics (Fig. 2.9, bottom left), the operating field of the turbocharger in the compressor map is determined at the various operating points, such as LET, maximum torque, design point, and nominal power of the engine. At any operating point, the required mass flow rate of the charge air at the given turbocharger speed results from the engine power according to Eqs. (1.1 and 1.2). Additionally, the necessary charge-air density is given by Eq. (1.3). The compression ratio without air intercoolers is calculated from Eq. (1.10). In case of using air intercoolers (see Fig. 2.10), the charge-air temperature T_2 drops at a lower temperature T_{2*} leading to the increase of the charge-air density ρ_{2*} .

The charge-air temperature T_{2*} after the intercooler is calculated from the compressed charge-air temperature T_2 , coolant inlet temperature T_c , and intercooler efficiency ε_c (usually between 0.6 and 0.8) as

$$T_{2*} = (1 - \varepsilon_c)T_2 + \varepsilon_c T_c < T_2 \quad (2.27)$$

Thus, the charge-air temperature in case of using air intercoolers drops with

$$\begin{aligned} \Delta T_{2*} &\equiv T_{2*} - T_2 \\ &= \varepsilon_c (T_c - T_2) < 0 \end{aligned} \quad (2.28)$$

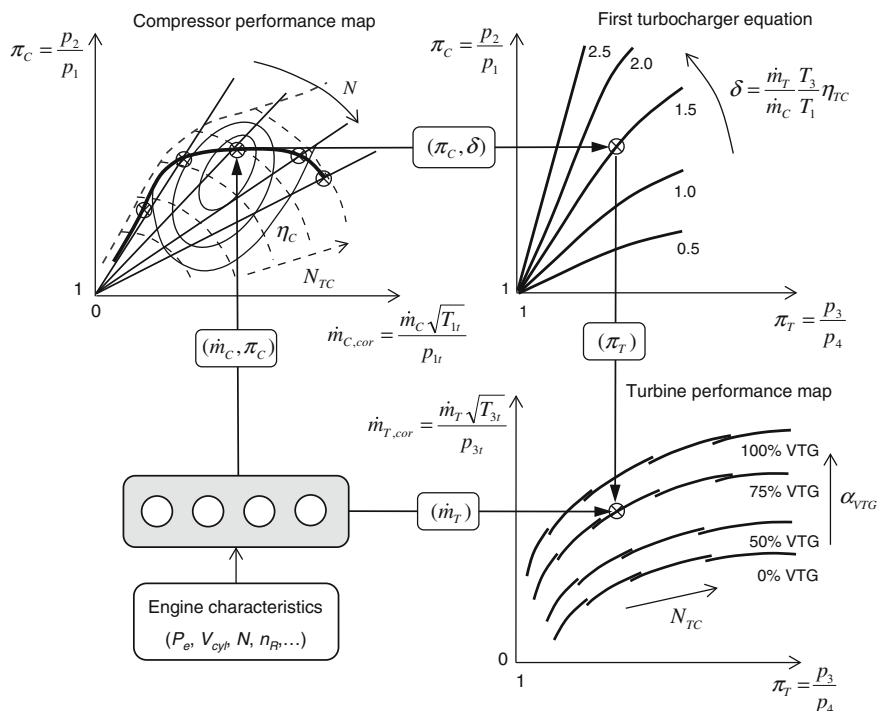


Fig. 2.9 Matching procedure of turbochargers

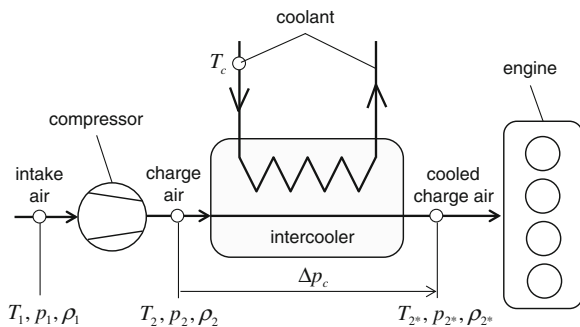


Fig. 2.10 Compressor using a charge-air intercooler

Therefore, the charge-air density rises from ρ_2 to ρ_2 at a small pressure drop in the intercooler. Using the state equation of a perfect gas, the charge-air density is calculated as

$$\rho_{2^*} = \frac{p_{2^*}}{R_a T_{2^*}} = \frac{p_2 - \Delta p_c}{R_a T_{2^*}} > \rho_2 \quad (2.29)$$

where Δp_c is the pressure drop in the air intercooler.

Substituting Eqs. (1.9, 2.27, and 2.29), one obtains the compression ratio of the compressor in case of using the air intercooler

$$\begin{aligned} \pi_c &= \frac{p_2}{p_1} = \frac{p_{2^*} + \Delta p_c}{p_1} = \frac{\rho_{2^*} R_a T_{2^*} + \Delta p_c}{p_1} \\ &= \frac{\rho_{2^*} R_a \left[(1 - \varepsilon_c) T_1 \left(1 + \frac{1}{\eta_c} \left(\pi_c^{\left(\frac{\kappa-1}{\kappa} \right)_a} - 1 \right) \right) + \varepsilon_c T_c \right] + \Delta p_c}{p_1} \end{aligned} \quad (2.30)$$

where the charge-air density ρ_{2^*} is given by the engine requirement and $\kappa_a \approx 1.4$ is the isentropic exponent of the charge air.

The charge-air density ρ_{2^*} is determined by iteratively solving Eq. (2.30) under the given boundary conditions for the engine, compressor, and intercooler.

(2) The operating point of the turbocharger is located in the compressor performance map (Fig. 2.9, top left) at the given mass flow rate and compression ratio of the charge air that have been computed in the step 1. The value δ in the diagram of the first turbocharger equation involves the mass flow rates of the charge air and exhaust gas, the temperatures of the exhaust gas and intake air, and the turbocharger efficiency. It results from the operating condition of the engine and the guessed/measured efficiency of the turbocharger.

(3) From the given compression ratio π_c and value δ , the expansion ratio π_T of the turbine corresponding to the operating point is determined in the diagram of the first turbocharger equation (Fig. 2.9, top right).

(4) Both mass flow rate and expansion ratio of the turbine given in the steps 2 and 3 are used to determine the operating point of the turbocharger in the turbine performance map (Fig. 2.9, bottom right).

The operating point gives the corresponding VTG angular position of 75 % VTG. Note that the mass flow rate of the exhaust gas that is identical with the mass flow rate of the VTG turbine, equals the mass flow rates of the charge air and injected fuel in the cylinders based on the air–fuel ratio AFR defined in Eq. (1.2). Therefore, the mass flow rate of the exhaust gas is written as

$$\dot{m}_T = \dot{m}_a + \dot{m}_f = \dot{m}_a \left(\frac{AFR + 1}{AFR} \right) \quad (2.31)$$

Using the turbomachinery theory, the outflow diameter D_2 (exducer diameter) of the compressor wheel and the inflow diameter D_3 (inducer diameter) of the turbine wheel are computed at the given effective powers and mass flow rates of the compressor and turbine, mechanical efficiency, and turbocharger speed. The matching procedure of turbochargers is iterated until the guessed values, such as the

efficiencies of the compressor and turbine, efficiency of the air intercooler, etc., are converged. Furthermore, the computed values could be rematched with the measured efficiencies as soon as they are available.

References

1. Aungier, R.H.: Turbine Aerodynamics. ASME Press, New York (2006)
2. Baines, N.C.: Fundamentals of Turbocharging. Concepts ETI, Inc, Wilder (2005)
3. Cumpsty, N.A.: Compressor Aerodynamics. Krieger Publishing Company, Melbourne (2004)
4. Heywood, J.B.: Internal Combustion Engine Fundamentals. McGraw-Hill, New York (1988)
5. Japikse, D., Baines, N.C.: Introduction to Turbomachinery. Concepts ETI, Inc, Wilder (1994)
6. Japikse, D., et al.: Axial and Radial Turbines. Concepts ETI Inc, Wilder (2003)
7. Whitfield, A., Baines, N.C.: Design of Radial Turbomachines. Pearson Education, Longman Scientific and Technical (1990)

Rotordynamics of Automotive Turbochargers

Nguyen-Schäfer, H.

2015, XV, 362 p. 222 illus., 6 illus. in color., Hardcover

ISBN: 978-3-319-17643-7